Available online at www.sciencedirect.com
ScienceDirect
Energy Reports 8 (2022) 848–856
www.elsevier.com/locate/egyr

2022 The 5th International Conference on Renewable Energy and Environment Engineering (REEE 2022), 24–26 August 2022, Brest, France

Thermal management of refrigeration unit for electric refrigerated vans: An experimental case study

Anita Aliu[a], Mohammad-Sofi Imran[a], Truong Quang Dinh[a,*], Jongil Yoon[b]

[a] *WMG, University of Warwick, Coventry, United Kingdom*
[b] *KOCETI, Korea Construction Equipment Technology Institute, South Korea*

Received 6 October 2022; accepted 10 October 2022
Available online xxxx

Abstract

In future, electric vehicles are expected to be adopted in the food transport to aid addressing limited access to fossil fuel and reduce greenhouse gas emission. However, their construction has to include consideration of a Temperature Refrigeration Unit (TRU) that is used to transport foods at low temperatures without significantly impacting the vehicle's operation or driving range. In this paper, we investigate the benefit of implementing Model Predictive Control (MPC) in a thermal management system (TMS) of a TRU for electric vans. A comparative study between the developed MPC-based TMS and the traditional proportional–integral (PI) - based TMS has been carried out using a physical thermal rig. The experimental results show up to 43% energy savings could be achieved by the MPC, compared to the case using the PI strategy.

Peer-review under responsibility of the scientific committee of the 5th International Conference on Renewable Energy and Environment Engineering, REEE, 2022.

Keywords: Temperature Refrigeration Unit; Electric van; Model Predictive Control; Thermal management system

1. Introduction

The global lockdown that occurred in 2019 and the subsequent activities that came after economies started opening up have resulted in significant increase in fossil fuel prices. This has also affected the cost of food transport. One solution is to adopt electric vehicles (EV)s in the commercial food transportation sector. Another reason for adopting commercial EVs is highlighted by Tassou et al. [1], indicating that commercial ICE vehicles commonly employed in food transportation can account for 40% of the total greenhouse gas emissions. Consequently, commercial EVs can contribute to addressing concerns about the limited access to fossil fuels, decarbonization in the transportation sector to maintain the global target, rise in temperature below 2 °C [2].

Overwhelming concerns when designing EVs are power–energy consumption and maintaining the optimal operating temperature as EVs are used in different climate and environmental conditions [3]. These concerns are

* Corresponding author.
E-mail address: T.Dinh@warwick.ac.uk (T.Q. Dinh).

https://doi.org/10.1016/j.egyr.2022.10.269

Peer-review under responsibility of the scientific committee of the 5th International Conference on Renewable Energy and Environment Engineering, REEE, 2022.

mainly due to interaction between the battery and the vehicle powertrain forming intricate feedback loops with other components of the vehicle [4] which impacts the vehicle driving range. In commercial EVs used for food transportation, additional components especially Temperature Refrigeration Units (TRUs) are integrated to maintain the quality and integrity of goods, subsequently further impacting the driving range. Therefore, the TRU operation has to be considered in designing vehicle control schemes to maintain an optimal vehicle operation.

Most of the studies focused on energy and/or thermal management systems in the literature are for passenger use EVs [5]. A heuristic real-time control approach is adopted by Kim et al. [4] in designing a battery thermal management system (BTMS) to improve the efficiency and reliability of EV batteries. However, such approach could not offer an optimal thermal management performance, in terms of efficiency and reliability. To address this drawback more advanced techniques have been utilized by other researchers. For example, dynamic programming (DP) approach is applied to the BTMS of a Toyota RAV4 EV to trade-off between energy savings and battery usage [6]. Although DP could offer good controller performance as state constraints are easily incorporated in the design of the BTMS, it is not a practical option for real-time implementation due to the computational complexity in solving the optimization problem. In another study, Pontryagin's maximum principle (PMP) is used to optimize BTMS of an EV which is more convenient in terms of requiring differential equations to be solved to find the optimum [7]. Nevertheless, PMP-based approach requires efforts in tuning co-states in the Hamiltonian for different driving conditions to obtain an optimal solution. Both the DP and PMP techniques therefore require a full knowledge of driving cycles in solving optimization problems. One approach explored to address these issues is the use of controllers based on model predictive control (MPC). Different to DP or PMP, MPC is an online optimization strategy which is based on only the instantaneous system state measurements and a prediction horizon to derive an optimal control decision. MPC therefore gains interest in engineering research communities, and the automotive industry is one of the fields where MPC techniques are rapidly becoming exceedingly popular [8].

In recent years, MPC has been exploited in the design of energy and thermal management strategies for hybrid/electric vehicles. This includes research on either cabin thermal management [8,9] or battery thermal management [10,11] or integrated cabin-battery thermal management [12–14]. These aforementioned TMS works are adequate for passenger EVs. To the best of the authors knowledge, no thermal management optimization strategy is proposed for TRU operation on commercial EVs. In this paper we aim at formulating an MPC solution to TMS for a TRU test rig for an electric van that minimizes energy consumption, taking into account the door operation and ambient temperature. The performance of the MPC is compared to the classical proportional–integral (PI) control. We use PI as a benchmark for comparison as it would typically represent a more traditional approach to evaluating controller and for its proven applicability in industrial control systems. In both controllers, the only manipulated input is the compressor load factor which influences the speed of the compressor. However, due to the flexibility of the MPC formulation, manipulation of factors such as compressor and TRU temperature rate of change, and target temperature tracking are explicitly incorporated. The effect of such inputs and constraints in the thermal dynamics are derived in the next section, which are used to formulate the MPC problem.

The rest of the paper is organized as follows. A simplified model of the TRU is presented in Section 2. Section 3 states the optimal problem formulation together with set points and constraints, which are used in the formulation of the MPC in Section 4. Section 5 presents the results from implementing the controller on the TRU test rig. Finally, the concluding remarks are summarized in Section 6.

2. Temperature refrigeration unit energy model

The overall schematic of a Temperature Refrigeration Unit illustrating the energy flow between a thermal compartment and a loop consisting of a compressor, condenser, and evaporator, is shown in Fig. 1.

To develop the TRU model for the targeted refrigeration unit on-board a commercial electric van, a representative model is developed within MATLAB/Simulink environment with the parameters of the TRU given in Table 1. The dynamics of the TRU whose temperature is maintained by an evaporator and condenser fan, and a compressor are described by the following equations based on energy balance principle. The cooling power delivered to the TRU from compressor is given by:

$$P_{cool} = -1000 L_{comp} \, \mathrm{P}_{rated} \, \eta_{cool} \tag{1}$$

The speed of the compressor is determined by the compressor load factor denoted as L_{comp}. The compressor rated power and cooling efficiency are denoted as P_{rated} and η_{cool} respectively. The TRU temperature, denoted as T_{TRU},

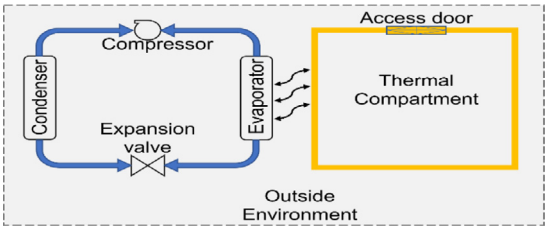

Fig. 1. Schematic diagram of simple thermal refrigeration circuit.

Table 1. TRU model parameters.

Parameters	Symbol	Value	Units
Compartment insulation			
Insulator U-Value	U_{insul}	1.5	$\frac{W}{m^2K}$
Cooling system			
Cooling efficiency	η_{cool}	85	%
Compressor rated power	P_{rated}	1.5	kW
Evaporator fans maximum current	I_{max}	13	A
Number of evaporator fans	N_{evap_fan}	1	–
Condenser fans maximum current	I_{max}	13	A
Number of condenser fans	N_{cond_fan}	1	–
Cooling system operation voltage	V_{oper}	12	V
Allowed heating hysteresis	τ	2	°C
Compartment geometrical			
Total surface area	SA_{total}	13.61928	m^2
Total Volume	V_{comp}	3.301488	m^3
Air parameters			
Air density	ρ_{air}	1.225	$\frac{kg}{m^3}$
Air specific heat capacity	C_{air}	1	$\frac{kJ}{kg\ K}$
Ambient temperature	T_{out}	15	°C
Allowable temperature hysteresis	τ	2	°C
Data based parametrization			
Mass and specific heat capacity	$m.C_p$	32	$\frac{kJ}{K}$
Average service load coefficient	SL	0.12	–

influences heat exchange between the TRU compartment walls due to the different temperature outside and inside of the compartment. This is calculated using the outdoor convective heat load formula (2). Hence, the net cooling power can be determined using (3).

$$\dot{Q}_{\text{cov}} = SA_{total} U_{insul} \left(T_{out} - T_{TRU}\right) \tag{2}$$

$$P_{cool\_net} = \dot{Q}_{\text{cov}} + P_{cool} \tag{3}$$

The opening and closing of the TRU door will also influence T_{TRU}. This is because the air inside and outside the TRU changes when the door is open which causes the air temperature inside the compartment to increase. This air volume heat change is estimated by:

$$\dot{Q}_{vol\_chg} = \left[1000.SL.V_{comp}.\rho_{air}.C_{air}\left(T_{out} - T_{TRU}\right)\right] D_{OC} \tag{4}$$

where D_{OC} denotes the TRU door opening and closing operation. D_{OC} is assigned a value of 1 when the door is opened and 0 when the door is closed. SL is the average service load coefficient, V_{comp} is the volume of the TRU compartment, ρ_{air} is the air density and C_{air} is the air specific heat capacity.

The compressor will be expected to turn on or off when T_{TRU} is outside certain limits. The time during which the compressor is on has to be calculated so that T_{TRU} between sampling instances can be estimated. This cooling time, t_{cool}, is estimated using the logic:

if $P_{cool\_net} == 0$ **then**

$$t_{cool} = T_s$$

else if $\left(T_s > \left(T_{t\,\arg} - T_{TRU}\right) * \frac{1000^* m.C_p}{P_{cool\_net}}\right)$ && $\left(\left(T_{t\,\arg} - T_{TRU}\right) * \frac{1000^* m.C_p}{P_{cool\_net}} > 0\right)$ **then**

$$t_{cool} = T_s$$

else

$$t_{cool} = \left(T_{t\,\arg} - T_{TRU}\right) * \frac{1000^* m.C_p}{P_{cool\_net}}$$

end if

Sampling time is denoted as T_s and $T_{t\,\arg}$ denotes the target temperature of the TRU. The mass and specific heat capacity of the goods and interior air of the TRU is denoted as $m.C_p$. The change in T_{TRU} between sampling instances is calculated using (5). Hence, the T_{TRU} at the next sampling instant is determined using (6).

$$\Delta T_{TRU} = \frac{\left[\frac{P_{cool\_net} t_{cool}}{1000} + \frac{\dot{Q}_{vol\_chg}}{1000}\right]}{m.C_p} \tag{5}$$

$$T_{TRU}(t+1) = T_{TRU}(t) + \Delta T_{TRU} \tag{6}$$

The energy consumed by the TRU (E_{TRU}) at each time instant can be calculated by adding up the fan energy demand (E_{fan}) with the compressor energy demand (E_{comp}) (12). However, E_{comp} depends on the power of the evaporator fan (P_{evap_fan}) and that of the condenser fan (P_{cond_fan}), and the energy consumed by the fans (E_{fan}) and compressor (E_{comp}) at each time instant. The equation for calculating P_{evap_fan} and P_{cond_fan} are respectively shown in (7) and (8) with N_{evap_fan} and N_{cond_fan} been the respective number of fans installed. I_{max} is the maximum rated current for the fan and V_{oper} is the cooling system operating voltage. The total power consumed by the fan is shown in (9). The equation for calculating E_{fan} and E_{comp} are shown in (10) and (11) respectively.

$$P_{evap\_fan} = N_{evap\_fan}\ \mathrm{I}_{\max} V_{oper} \tag{7}$$

$$P_{cond\_fan} = N_{cond\_fan}\ \mathrm{I}_{\max} V_{oper} \tag{8}$$

$$P_{fan} = P_{evap\_fan} + P_{cond\_fan} \tag{9}$$

$$E_{fan} = \frac{P_{fan}(t) - P_{fan}(t-1)}{2} * \frac{t - (t-1)}{3600} \tag{10}$$

$$E_{comp} = \left[-\frac{P_{cool} t_{cool}}{3600}\right] \eta_{cool} \tag{11}$$

$$E_{TRU} = E_{fan} + E_{comp} \tag{12}$$

The total energy consumed by the TRU can be calculated by adding up the accumulated fan and compressor energy demands as shown in (13). The divisions by 1000 is to convert from Wh to kWh.

$$\sum E_{TRU} = \sum \frac{E_{fan}}{1000} + \sum \frac{E_{comp}}{1000} \tag{13}$$

3. Constrained optimal control problem formulation

3.1. Set points and cost function

In this paper, we aim at formulating an optimal control problem to TMS for the TRU that minimizes its fuel consumption and ensure safe operation of the compressor, taking into account disturbances such as the TRU door open/close operation and ambient temperature. To this end, the manipulated input is L_{comp}, which controls the speed

of the compressor. The effect of the manipulated input in the overall TRU dynamics where derived in the previous section, in which the TRU model was obtained based on information from the project partner and first principle. Input signal T_{trag} and disturbances D_{OC} and T_{out} are artificial signals generated based on the required experimental environment.

The overall stage cost $J(t)$ to be minimized within the optimal control problem is defined as

$$J(t) = w_\pi L_{comp}(t) + w_\beta \left[T_{TRU}(t) - T_{trag}(t)\right]^2 + w_\gamma \left[\Delta T_{TRU}(t)\right]^2 \tag{14}$$

where w_π, w_β and w_γ are weights which can be constant or time varying. $\Delta T_{TRU}(t) = T_{TRU}(t) - T_{TRU}(t-1)$ denote the TRU temperature change between sampling instant and a weight on this change allows one to admit larger variations of the TRU temperature over the period the EV is in operation.

3.2. Constraints

Input $L_{comp}(t)$ is generated under the constraint (15) while T_{TRU} is constrained between the limits shown in (16)

$$0(0\%) \leq Lcomp(t) \leq 1(100\%) \tag{15}$$

$$T_{TRU}^{\min} \leq T_{TRU}(t) \leq T_{TRU}^{\max} \tag{16}$$

The maximum allowed limit of P_{cool} is constrained by the compressor rated power i.e., $P_{cool} \leq \mathrm{P}_{rated}$.

4. Model predictive control formulation

The control problem at time t can be stated as follows: Given the current fan power P_{fan}, the accumulated energy consumed by the TRU $\sum E_{TRU}$ and its current temperature T_{TRU}, maintain T_{TRU} at or around T_{trag} while maintaining ΔT_{TRU} at admissible levels and the compressor controlled at reasonable speed. This is achieved by manipulation of L_{comp} which influences P_{cool}, considering the disturbances D_{OC} and T_{out}. The selection of L_{comp} is based on the compromised between the different weights in the cost function. To achieve the TRU objective, the MPC problem is formulated over a finite-time horizon N_H considering sampling time T_S:

$$\min_{\mathbf{L}_{comp}} J(k) = \sum_{i=\mathbf{0}}^{N_H} \left[\mathbf{w}_\pi L_{comp}(i|t) + \mathbf{w}_\beta \left[T_{TRU}(i|t) - T_{trag}(i|t)\right]^{\mathbf{2}} + \mathbf{w}_\gamma \left[\Delta T_{TRU}(i|t)\right]^{\mathbf{2}}\right] \tag{17}$$

$$\textit{subject to}$$

$$(1)\text{–}(13),\ (15),\ (16)$$

$$T_{t\,\arg}(i|k) - \tau(i|k) \leq T_{TRU}(i|k) \leq T_{trag}(i|k) + \tau(i|k)$$

$$L_{comp}(0|k) w_{comp}^{\min} \leq w_{comp} \leq L_{comp}(0|k) w_{comp}^{\max}$$

where the predicted value at a time instant $k+i$ when a prediction is made at time instant k is denoted as $(i|k)$. The quadratic term $\left[T_{TRU}(i|t) - T_{trag}(i|t)\right]^2$ is used to enforce the TRU temperature reference tracking, while $[\Delta T_{TRU}(i|t)]^2$ maintains the TRU temperature over time. The penalty weights on these terms are denoted by w_β and w_γ respectively, w_π is the weight imposed on the manipulated variable $L_{comp}(i|k)$. To eliminate the possibility of (17) being infeasible, the lower and upper TRU temperature limits are both set to $T_{t\,\arg}$ plus hysteresis (τ). This ensures T_{TRU} will never deviate far from $T_{t\,\arg}$ during the TRU operation. The MPC feedback law is defined by the first element $L_{comp}(0|k)$ of the optimal solution sequence to (17) obtained from $\mathbf{L}_{comp} = L_{comp}(0|k), L_{comp}(1|k), \ldots, L_{comp}(N_H|k)_{i=0}^{N_H}$. In the experimental setup, the compressor speed is not allowed to run at its maximum allowed limit or to completely turn off. Hence, limitations are placed on the compressor speed as shown in (17). The MPC simulation is carried out on a desktop computer, with an Intel Core GHz processor, in MATLAB/SIMULINK using fmincon for formulating the problem.

5. Analysis

This section describes the experimental setup of the thermal test rig and software used. Also, the performance of the designed controllers based on different prioritizes are investigated, specifically those with ensure the best performance of the TMS. The investigation considers three cases and compares their performance against each other.

5.1. Experimental setup

A High Voltage Air Conditioning (HVAC) test rig is used to test both the PID and MPC controllers. The experimental setup showing the HVAC test rig and its connection to a PC is shown in Fig. 2. A section of the HVAC test rig is used to emulate the operation of a TRU. The HVAC rig is enclosed within a thermal chamber. The thermal chamber helps to simulate the ambient environment surrounding an electric van in motion by maintaining a relatively constant airflow rate, humidity, and ambient temperature. To offer the similar operating range as in an EV,

The HVAC rig is powered by an 80 kW 440 V DC power supply. Connection to the thermal chamber and HVAC rig is established using a VT system from Vector Informatik GmbH used as the system real-time (RT) simulator and CANoe a tool for the design and development of distributed systems. The HVAC rig has a butterfly valve used to emulate the opening/closing operation of a door on a commercial TRU to access its enclosed compartment. The butterfly valve is opened and closed using a 3-min interval. The butterfly valve is accessed through the thermal chamber double door.

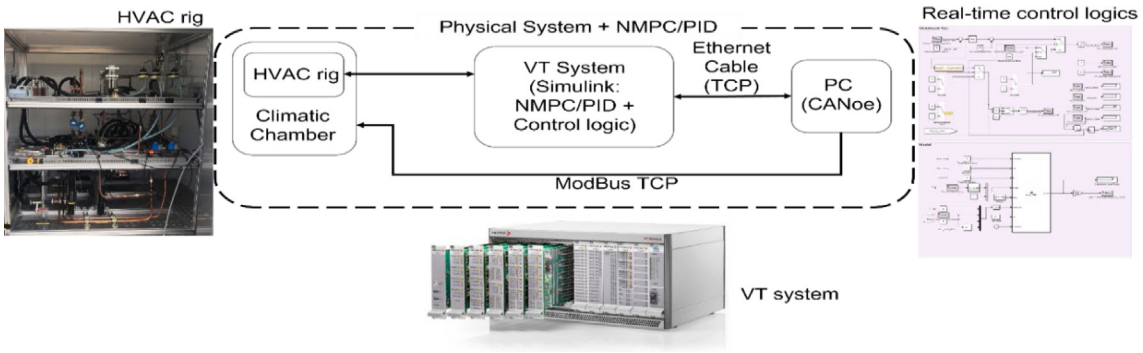

Fig. 2. Layout of the real-time control system setup.

The airflow rate, humidity and ambient temperature are set to 426 $^{m^3}/_h$, 80% and 12 °C respectively via a Human Machine Interface (HMI) panel or through Simulink. The simulation setup window within the Vector CANoe software is configured with 1 controller area network (CAN) and 4 local interconnect network (LIN) channel. The CAN channel connects the thermocouples while the LIN channels connects the compressor, cabin, EDU, and battery. These channels enable communication between the controller in Simulink and the HVAC rig through the VT system. However, for this experiment only 2 LIN channels used, the compressor and cabin. The cabin is used to emulate the refrigeration system and for safety, the compressor speed w_{comp} is limited between 800 and 2000 revolutions per minute.

5.2. Results

The target ambient temperature of the thermal chamber surrounding the test rig is set to 12 °C. However, the thermal chamber temperature is allowed to deviate around this value as maintaining constant target ambient temperature for the duration of the experiment is quite challenging. The resulting temperature profile of the thermal chamber is shown in Fig. 3. The types and parameters of the controllers implemented within the TMS as shown in Table 2. Case 1 shows the proportional and integral gains $\left(K_p \text{ and } K_I\right)$ of the PI controller implemented within the TMS.

The gains are set to prioritize T_{TRU} achieving the target temperature as soon as possible. Case 2 and 3 shows two set of values for the weights of the MPC objective function within the TMS. Weights of Case 2 are set to prioritize minimizing energy consumed via regulating the compressor speed as only the value wπ is set. In Case 3, the weights set exploits the trade-off between energy consumed by the compressor, target temperature tracking and temperature variation between sampling instances, with high priority given to temperature tracking. The resulting operation of the compressor with the controller setting shown in Table 2 when implemented in the TMS are shown

Table 2. Controller parameters.

Case	Controller	Parameter
Case 1	PI	$K_p = 500$; $K_I = 10$
Case 2	MPC	$[w_\pi w_\beta \omega_\gamma] = [2000]$
Case 3	MPC	$[w_\pi w_\beta \omega_\gamma] = [51005]$

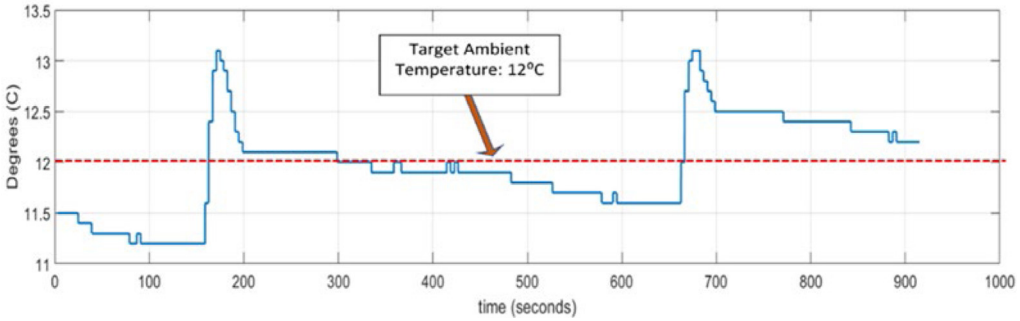

Fig. 3. Ambient temperature profile of the thermal chamber.

in Fig. 3. The resulting T_{TRU} profile obtained after the implementation of each controller are shown in Fig. 5. The 3-min intervals when the butterfly valves are open to emulate the open/close operation of a TRU door to access its compartment for loading and off-loading are marked as Load 1 and 2 in the plots in Figs. 4 and 5. It can be observed in Fig. 3a that a significant change in the compressor operation is noticed in Case 1 when the butterfly valve is open. In this case, the priority is to achieve the target temperature as soon as possible. This results in significant overshoot when T_{TRU} is between 0 °C and the upper limit of 2 °C. The overshoot continues except during the two 3-min interval when the butterfly valve is open. This is because the air within the thermal chamber directly affects the T_{TRU} when the valve is open, and the compressor remains on, thereby work harder, to keep T_{TRU} close to the allowed upper limit of 2 °C and to compensate for temperature change between air inside and outside the compartment. The resulting T_{TRU} profile is shown in Fig. 5a.

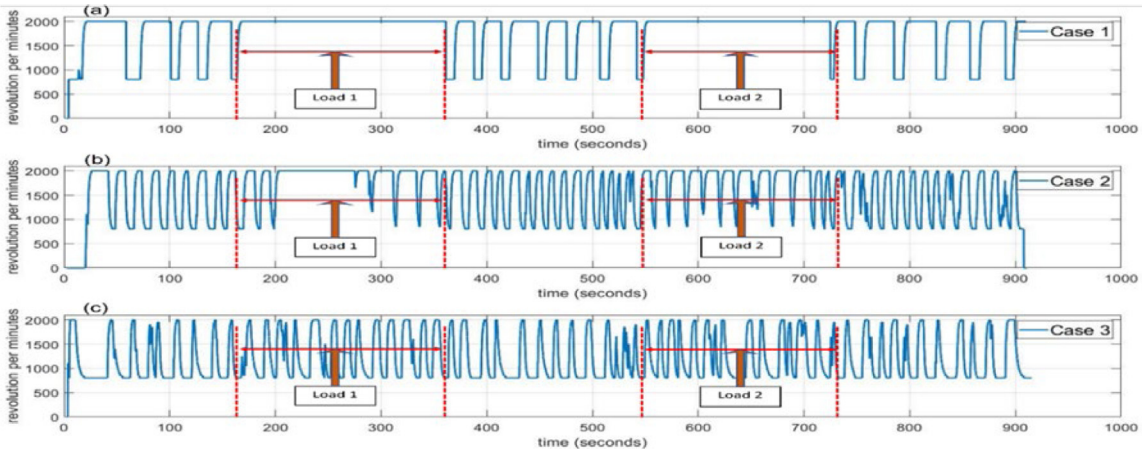

Fig. 4. Compressor speed after implementing each controller in the TMS.

Fig. 4b, shows the compressor operation when the MPC of Case 2 was implemented in the TMS. It can be observed that during the period when the butterfly valve is open the compressor does not work as much as in Fig. 4a. This is because the only penalty imposed in the objective function is on L_{comp}, prioritizing minimizing the compressor operation so that it does not consume much energy. In general, as the compressor operation in Fig. 4b

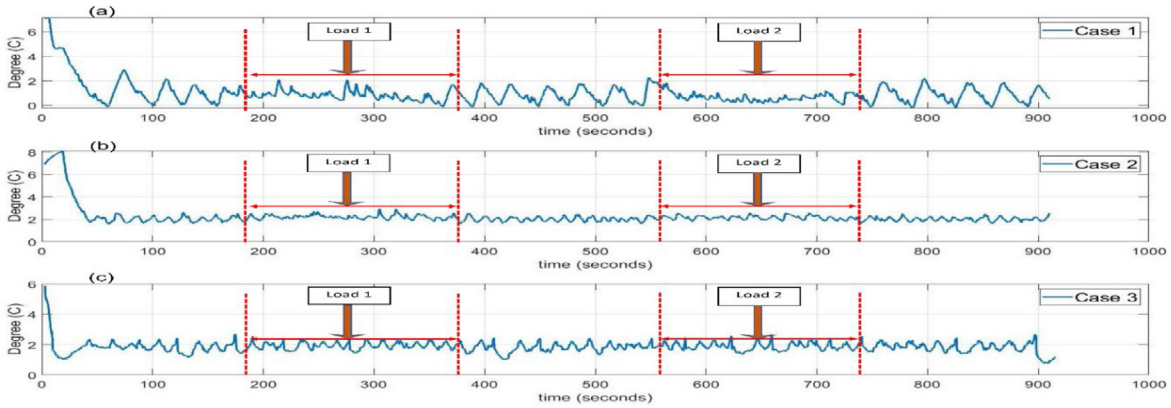

Fig. 5. TRU temperature after implementing each controller in the TMS.

does not stay on over long periods as in Fig. 4a, T_{TRU} profile in Fig. 5b does not deviate and overshoot the upper limit as observed in Fig. 5a.

In Case 3, penalties are imposed on all weights in the cost function however, the penalty is heavier on the difference between T_{TRU} and T_{trag}. Compared to the compressor operation observed in Fig. 4a and b during the periods when the butterfly valve is open, no noticeable change is observed in the compressor operation in Fig. 4c and in the resulting TTRU profile in Fig. 5c. As the compressor operation reduces in each case, it is unsurprising to see that the accumulated energy consumed by the compressor in Case 3 is less than in Case 2 and Case 1. The accumulated energy consumed by the compressor in each case are shown in Table 3. It is worth highlighting that the significant energy saving achieved in Case 3 can be attributed to the difficulty in completely maintaining the ambient temperature in the thermal chamber. In Case 3, the ambient temperature settled between 9 °C and 11 °C. However, it is maintained that significant savings can still be achieved if the ambient temperature shown in Fig. 3 was achieved.

Table 3. Accumulated energy consumed by the compressor.

Case	Controller	Energy	Savings compared	
			To Case 1	To Case 2
Case 1	PI	340 kJ	–	–
Case 2	MPC	305 kJ	∼10%	–
Case 3	MPC	175 kJ	∼48%	∼43%

6. Conclusion and future work

This paper focused on the development of TMS for a TRU in an electric van. As the refrigeration unit is expected to draw power from the onboard high voltage battery, a control scheme that ensures minimal energy is consumed by the compressor will be beneficial. To this end, this paper investigates PI and MPC implementation in TMS for a TRU. The MPC implementation results in both better energy savings and compressor operation, especially in the case where the weights in the objective function are set to exploit trade-off between energy consumed by the compressor, achieving target temperature tracking and minimizing temperature variation between sampling instances. Due to the complexity of the MPC scheme, future work needs to be considered on the development of an adaptive MPC scheme but with less computational cost with possible inclusion of temperature hysteresis in the objective function. In addition, future development of the TMS should consider online forecasting technique to better understand how change in ambient temperature affects the TRU operation

Declaration of competing interest

The authors declare that they have no known competing financial interests or personal relationships that could have appeared to influence the work reported in this paper.

Data availability

The authors do not have permission to share data.

Acknowledgments

This work is supported by the Warwick Manufacturing Group - High Value Manufacturing Catapult, Cit-E-Van project (project no. 10006082)

References

[1] Tassou SA, De-Lille G, Ge YT. Food transport refrigeration – Approaches to reduce energy consumption and environmental impacts of road transport. Appl Therm Eng 2009;29:1467–77.
[2] Santos G. Road transport and CO2 emissions: What are the challenges? Transp Policy 2017;59:71–4.
[3] Mali V, Saxena R, Kumar K, Kalam A, Tripathi B. Review on battery thermal management systems for energy-efficient electric vehicles. Renew Sustain Energy Rev 2021;151.
[4] Kim E, Shin KG. Real-time battery thermal management for electric vehicles. In: Int. conference on cyber- physical systems. 2014, p. 2013–5.
[5] Liang K, Wang M, Gao C, Dong B, Feng C, Zhou X, Liu J. Advances and challenges of integrated thermal management technologies for pure electric vehicles. Sustain Energy Technol Assess 2021;46:101–19.
[6] Masoudi Y, Mozaffari A, Azad NL. Battery thermal management of electric vehicles: An optimal control approach. In: ASME 2015 dynamic systems and control conference, Vol. 1. 2015, p. 1–7.
[7] Bauer S, Suchaneck A, Leon FP. Thermal and energy battery management optimization in electric vehicles using Pontryagin's maximum principle. J Power Sources 2014;246:808–18.
[8] Esen H, Tashiro T, Bernardini D, Bemporad A. Cabin heat thermal management in hybrid vehicles using model predictive control. In: 2014 22nd Mediterranean conference on control and automation, Vol. 210. 2014, p. 49—54.
[9] Wang H, Kolmanovsky I, Amini MR, Sun J. Model predictive climate control of connected and automated vehicles for improved energy efficiency. In: Proceedings of the American control conference, Vol. 2018. 2018, p. 828—833.
[10] Masoudi Y, Azad NL. MPC-based battery thermal management controller for Plug-in hybrid electric vehicles. In: Proceedings of the American control conference, Vol. 2017. 2017, p. 4365–70.
[11] Amini MR, Sun J, Kolmanovsky I. Two-layer model predictive battery thermal and energy management optimization for connected and automated electric vehicles. In: Proceedings of the IEEE conference on decision and control, Vol. 2018. 2019, p. 6976–81.
[12] Amini MR, Wang H, Gong X, Liao-McPherson D, Kolmanovsky I, Sun J. Cabin and battery thermal management of connected and automated HEVs for improved energy efficiency using hierarchical model predictive control. IEEE Trans Control Syst Technol 2020;28:1711–26.
[13] Amini MR, Kolmanovsky I, Sun J. Hierarchical MPC for robust eco-cooling of connected and automated vehicles and its application to electric vehicle battery thermal management. IEEE Trans Control Syst Technol 2021;29:316–28.
[14] Shafiei SE, Alleyne A. Model predictive control of hybrid thermal energy systems in transport refrigeration. Appl Therm Eng 2015;82:264–80.